The sea breeze/land breeze circulation in Los Angeles and its influence on nitryl chloride production in this region

N. L. Wagner,[1,2] T. P. Riedel,[3,4] J. M. Roberts,[1] J. A. Thornton,[3] W. M. Angevine,[1,2] E. J. Williams,[1,2] B. M. Lerner,[1,2] A. Vlasenko,[5] S. M. Li,[5] W. P. Dubé,[1,2] D. J. Coffman,[6] D. M. Bon,[1,2] J. A. de Gouw,[1,2] W. C. Kuster,[1,2] J. B. Gilman,[1,2] and S. S. Brown[1]

Received 21 March 2012; revised 6 September 2012; accepted 4 October 2012; published 27 November 2012.

[1] The sea breeze/land breeze diurnal circulation within the Los Angeles Basin and adjacent waters transports marine air into the basin during the day and urban air to Santa Monica Bay during the night. Nitryl chloride, $ClNO_2$ is a nocturnal trace gas formed from the heterogeneous reaction of dinitrogen pentaoxide (N_2O_5) with chloride containing aerosol. Its photolysis after sunrise produces atomic chlorine radicals and regenerates NO_2, both of which may increase ozone production. Mixing of the chloride source from marine sea salt with the urban NO_x source in Los Angeles provides conditions ideal for the production of $ClNO_2$. This paper presents an analysis using a wind profiler on the coast and measurements of $ClNO_2$ and its precursors made from both ship and aircraft to assess the prevailing meteorological conditions important for $ClNO_2$ production in this region, with a particular focus on the production over water within the land breeze phase of the circulation. A box model is used to calculate an upper limit to the amount of $ClNO_2$ capable of being produced strictly over Santa Monica Bay during the land breeze. On three out of the four nights of $ClNO_2$ measurements in Santa Monica Bay, the $ClNO_2$ exceeds the upper limit calculated using the box model and shows that the majority of the $ClNO_2$ is produced over the city and transported to Santa Monica Bay by the land breeze. This $ClNO_2$ transport suggests the sea breeze more efficiently transports aerosol chloride inland than land breeze transports NO_x offshore.

Citation: Wagner, N. L., et al. (2012), The sea breeze/land breeze circulation in Los Angeles and its influence on nitryl chloride production in this region, *J. Geophys. Res.*, *117*, D00V24, doi:10.1029/2012JD017810.

1. Introduction

[2] The diurnal sea breeze/land breeze circulation is a common and long-studied mesoscale phenomenon within the Los Angeles Basin. During daytime, a strong sea breeze brings air from the Pacific coast inland and transports pollutants from downtown Los Angeles eastward into the basin. The influence of this transport on air quality throughout the basin has been previously studied [e.g., *Gentner et al.*, 2009; *Washenfelder et al.*, 2011, and references therein]. During nighttime, a weaker land breeze transports urban emissions from the Los Angeles Basin over Santa Monica Bay [*Shair et al.*, 1982]. During late spring and summer, the land breeze typically begins at midnight and continues until well after sunrise, resulting in a 5–6 h period during which these urban air masses are transported over water in darkness. Nighttime chemical transformations can be important in determining the overall impact of the land breeze on air quality within the basin, especially since the products of these nighttime reactions are swept inland on the sea breeze during the following day and are known to be widely distributed throughout the basin [*Cass and Shair*, 1984]. The influence of this phase of the sea breeze/land breeze circulation has been less well studied, in part due to the smaller number of nighttime measurements over water, which have been limited to studies that have taken place either at the coast or at island sites [*Boucouvala et al.*, 2003].

[3] Of particular relevance to the sea breeze/land breeze circulation is the nighttime chemistry of nitrogen oxides, including the recently discovered nighttime chemical cycle that produces nitryl chloride ($ClNO_2$) [*Finlayson Pitts et al.*, 1989; *Osthoff et al.*, 2008]. This compound is formed from heterogeneous reactions of nitrogen oxides with chloride

[1]Earth System Research Laboratory, NOAA, Boulder, Colorado, USA.
[2]Cooperative Institute for Research in Environmental Sciences, University of Colorado Boulder, Boulder, Colorado, USA.
[3]Department of Atmospheric Sciences, University of Washington, Seattle, Washington, USA.
[4]Department of Chemistry, University of Washington, Seattle, Washington, USA.
[5]Air Quality Research Division, Science and Technology Branch Environment Canada, Toronto, Ontario, Canada.
[6]Pacific Marine Environmental Laboratory, NOAA, Seattle, Washington, USA.

Corresponding author: N. L. Wagner, Earth System Research Laboratory, NOAA, R/CSD7, 325 Broadway, Boulder, CO 80305, USA. (nick.wagner@noaa.gov)

0148-0227/12/2012JD017810

Table 1. This Analysis Used Measurements From the Instruments Listed in the Table Along With Their Detection Limits and References Describing the Measurement Techniques[a]

Species	Detection Limit	Method	Uncertainty (1σ)	Reference
		R/V Atlantis		
$ClNO_2$	5 pptv	I^- CIMS	±20%	*Kercher et al.* [2009]
N_2O_5	3 pptv	CRDS	±10%	*Wagner et al.* [2011]
DMS	18 pptv	PTR-ToF-MS	±13%	*Jordan et al.* [2009]
O_3	100 pptv	Chemiluminescence	±7%	*Williams et al.* [2006]
NO_2	14 pptv	Chemiluminescence	±4%	*Pollack et al.* [2010]
NO_y	50 pptv	Chemiluminescence	±13%	*Williams et al.* [2009]
VOCs	10 pptv	GC-FID	±10%	*Kuster et al.* [2004]
Surface area density		SMPS and APS	±55%	*Quinn et al.* [2002]
		NOAA P-3		
$ClNO_2$	50 pptv	I^- CIMS	±30%	*Osthoff et al.* [2008]

[a]I^- CIMS is Chemical Ionization Mass Spectrometry using iodine ion chemistry. CRDS is Cavity RingDown Spectrometer. PTR-ToF-MS is Proton Transfer Reaction Time-of-Flight Mass Spectrometer. GC-FID is Gas Chromatograph with a Flame Ionization Detector. SMPS is Scanning Mobility Particle Sizer. APS is Aerodynamic Particle Sizer.

containing aerosol (e.g., sea salt). It is photolyzed in the morning into atomic chlorine and nitrogen dioxide (NO_2). Both of these products have the potential to affect tropospheric chemistry and air quality: atomic chlorine radicals are strong oxidants that can initiate radical cycles through the oxidation of VOCs, and NO_2 is a component of NO_x, the catalyst that drives the production of ozone in the troposphere [*Chameides*, 1978]. Coproduction of both a radical source and NO_x in the morning hours has the potential to influence ozone production, especially in a highly polluted, VOC-rich region such as Los Angeles [*McLaren et al.*, 2010].

[4] $ClNO_2$ production begins with the reaction of O_3 and NO_2 (R1). NO_3 reacts further with NO_2 to form N_2O_5 which can thermally decompose to reform NO_3 (R2).

$$(R1) \qquad O_3 + NO_2 \rightarrow NO_3 + O_2$$

$$(R2) \qquad NO_3 + NO_2 \overset{M}{\rightleftharpoons} N_2O_5$$

[5] N_2O_5 reacts heterogeneously with aerosol to form nitric acid (HNO_3) or $ClNO_2$ with the relative branching determined by the aerosol chloride and liquid water content [*Bertram and Thornton*, 2009]. The source of chloride aerosol can come from the marine aerosol or from redistribution of chloride to other aerosol types via acid displacement and equilibrium repartitioning of gas phase hydrochloric acid (HCl). $ClNO_2$ chemistry has recently been found to be potentially responsible for a large portion of the total tropospheric atomic chlorine budget and to be produced in both coastal areas with chloride aerosol from sea salt [*Kercher et al.*, 2009; *Osthoff et al.*, 2008] and at a continental location far from the coast [*Mielke et al.*, 2011; *Thornton et al.*, 2010]. This nighttime halogen activation process is likely to be particularly important to air quality in the Los Angeles Basin, especially in the region in and around Santa Monica Bay. The outflow associated with the land breeze in that area contains large concentrations of both NO_x and ozone, and a source of chloride aerosol is available from sea spray over water. In this paper, we use field measurements to quantify the intensity, duration, and persistence of the land breeze. We further use chemical measurements associated with this land breeze to quantify $ClNO_2$ production over Santa Monica Bay. Radar wind profiler data on the coast is used to characterize the land breeze during the time period of the field intensive. Ship-based measurements of $ClNO_2$ and its precursors aboard the R/V Atlantis in Santa Monica Bay during the CalNex field intensive are reported. Chemical and meteorological observations are used in combination with a zero dimensional box model to constrain the amount of $ClNO_2$ capable of being produced strictly over water. During three of the four nights of $ClNO_2$ observations in Santa Monica Bay, this upper limit was lower than the observed $ClNO_2$ mixing ratios. This level of production is consistent with the $ClNO_2$ being produced not only over water but also over land in the residual boundary layer.

[6] The $ClNO_2$ measurements presented in this analysis were previously used by *Riedel et al.* [2012] in an analysis of chlorine emissions in the Los Angeles Basin. These analyses are expected to be complimented by future publications focusing on nocturnal measurements of NO_3, N_2O_5, HONO, and $ClNO_2$ collected during the CalNex field experiment at the Pasadena ground site and from the NOAA WP-3 aircraft.

2. Measurement Platforms and Techniques

[7] As part of the CalNex 2010 field experiment, the land breeze and $ClNO_2$ production were characterized using measurements from three platforms. A list of the instruments and the associated detection limits used in this analysis is shown in Table 1. Vertical profiles of wind speed and direction at the coast of Santa Monica Bay were measured at the Los Angeles International Airport (LAX) using a radar wind profiler. To characterize the land and sea breeze, this analysis uses data from the wind profiler for three months from 14 April 2010 until 11 July 2010.

[8] The R/V Atlantis was off the coast of California from 14 May to 8 June and was in Santa Monica Bay five nights during the land breeze on 15, 16, 21, 24, and 25 May 2010. Instruments aboard the R/V Atlantis measured meteorological variables as well as trace gases and aerosol chemical composition in the land breeze. In particular, a chemical ionization mass spectrometer was used for measurements of $ClNO_2$ [*Kercher et al.*, 2009]. N_2O_5 was detected using cavity ringdown spectrometry [*Wagner et al.*, 2011] and both O_3 and NO_2 were measured with a photolysis/chemiluminescence detector [*Williams et al.*, 2006]. All measurements

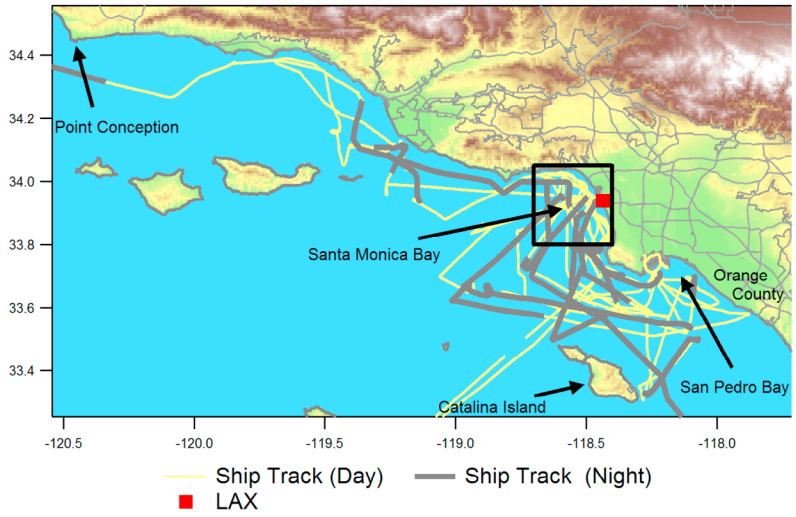

Figure 1. Map of Santa Monica Bay and the coast of Southern California with the track of the R/V Atlantis during CalNex. The ship track during the day is shown in yellow and during the night is shown in gray. LAX, the location wind profiler, and aircraft missed approaches is indicated by a red box. The black box is the region that was used to construct diurnal averages.

were made from the top of 10 m tower on the foredeck of the R/V Atlantis. The top of the tower was 17 m above the water surface.

[9] Several steps were taken to minimize and characterize the loss of N_2O_5 and its conversion to $ClNO_2$ on the walls of the 10 m inlet. Synthetic N_2O_5 was added to the inlet daily to measure the transmission of N_2O_5 as described in *Wagner et al.* [2011]. During the field measurements transmission of N_2O_5 was never less than 78% and was typically between 90% and 100%. During these N_2O_5 additions $ClNO_2$ was also measured and was less than 1% of the N_2O_5 concentration using new inlet tubing. After periods of high sea spray the conversion was as high as 10%. To avoid production of $ClNO_2$ in the inlet, the tubing was changed daily. The instrumented NOAA WP-3 made several flights over Los Angeles Basin and Santa Monica Bay. Four of these flights (30 May, 31 May, 2 June, and 3 June) were at night and were useful for characterization of the land breeze. Three of these flights included coastal vertical profiles from missed approaches to LAX.

[10] A map of Santa Monica Bay is shown in Figure 1. The yellow/gray trace shows the track of the R/V Atlantis during the day and night, and red square denotes LAX where the wind profiler is located and where NOAA P-3 missed approaches occurred. Diurnal averages for Santa Monica Bay were constructed from measurements while the R/V Atlantis was inside the black box indicated in Figure 1.

3. Meteorology of the Land Breeze

[11] A Doppler radar wind profiler is located at LAX and reports vertical profiles of wind velocity every hour. The wind profiler is located at 47 m above sea level (all heights are stated with respect to sea level) and only reports wind velocity for altitudes greater than 210 m. A diurnally averaged wind profile constructed using data collected between 14 April 2010 and 11 July 2010 is shown in Figure 2 as a color plot. The plot covers a 24 h time period beginning at 5 P.M. Pacific Daylight Time (PDT). The lowest row on the plot at 47 m shows diurnally averaged wind direction at the surface measured by a ground based anemometer and wind vane near the wind profiler.

[12] The sea breeze (blue) occurred below 700 m starting 11 A.M., approximately 5 h after sunrise and continues until 11 P.M. The land breeze (green-beige) developed at 11 P.M. initially at 500 m where there was little resistance from surface friction and continued after sunrise until 11 A.M. As the land breeze strengthened it spread down to 200 m (the lower limit of measurements from the wind profiler) two hours after it began. At the surface, the sea breeze weakened and the average winds were out of the south, approximately parallel to the shoreline, at the peak of the land breeze. Above 800 m were the prevailing regional winds (purple-red), which were from the northwest and did not undergo strong diurnal variation. The contours on the color plot indicate the persistence of the wind, which is the ratio of magnitude of the vector-averaged wind velocity to the scalar-averaged wind speed. The persistence ranges from 0 to 1 and represents the fraction of the time the instantaneous wind is in the direction of the average wind. The wind persistence was highest during the sea breeze, greater than 0.8. The direction was more erratic during the land breeze, indicated by a lower persistence of 0.4 to 0.6.

[13] The wind direction and speed measured at the surface aboard the R/V Atlantis were similar to observations from the LAX wind profiler. Figure 3 (top) shows the diurnally averaged wind direction and speed sampled 17 m above the surface aboard the R/V Atlantis. The R/V Atlantis was typically 1 to 15 km from the coast during these measurements. The land breeze was apparent as the wind direction shifted from west to east shortly after midnight and the wind speed dropped. Figure 3 (bottom) shows the surface winds near the shore (LAX). This diurnal average was constructed from 89 days of measurements from 14 April 2010 to 11 July 2010 (the same range as the radar wind profiler). At the surface the wind speed dropped during the night, but there was no

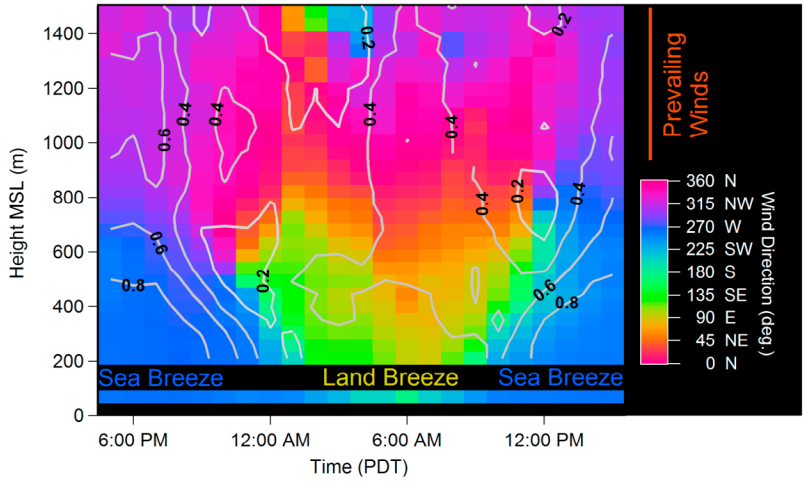

Figure 2. The averaged wind direction at LAX as a function of height and time of day. The sea breeze (blue) occurs in afternoon and early evening. The land breeze (green-beige) develops at midnight and continues for eleven hours until well after sunrise. Both the sea and land breeze occur in a layer extending up to 700 m. Above this layer the prevailing regional winds are from the north to northwest. The contours (gray) show the persistence of the wind which is the ratio of the vector average of the wind velocity to the scalar average of the wind speed. The persistence ranges from 0 (no preferred direction) to 1 (constant in one direction). The lowest line on the graph shows the diurnally averaged wind direction measured at the surface with an anemometer and wind vane.

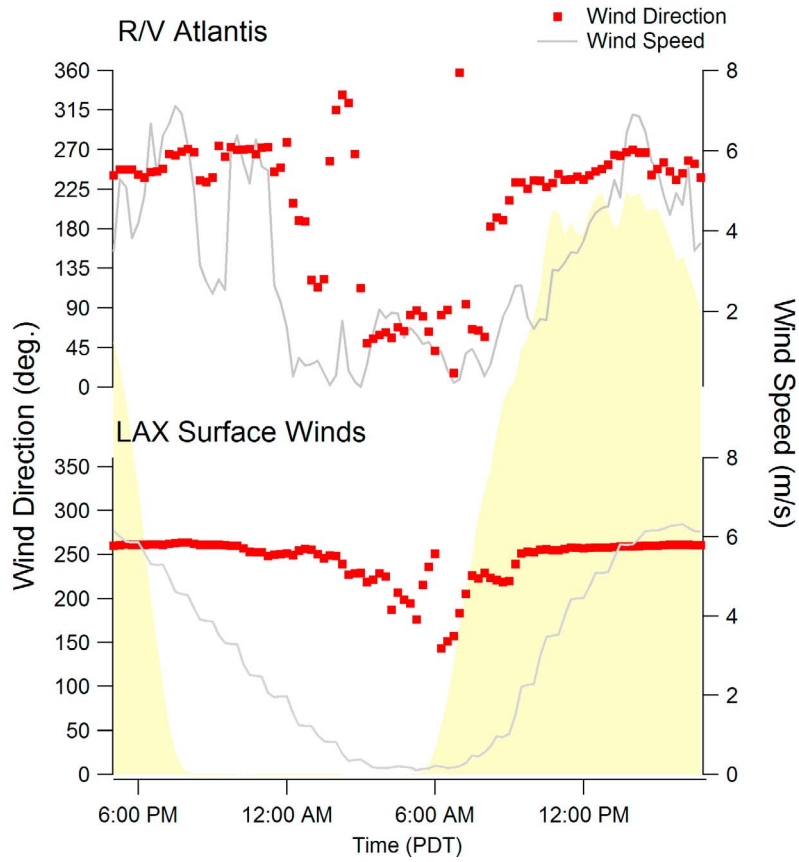

Figure 3. Diurnally averaged wind direction and speed measured during (top) 5 days aboard the R/V Atlantis and (bottom) over 3 months at the surface at LAX. Although, the easterly land breeze is evident in the winds observed from the R/V Atlantis, an easterly flow is not common enough to be seen in the long-term average surface winds at LAX.

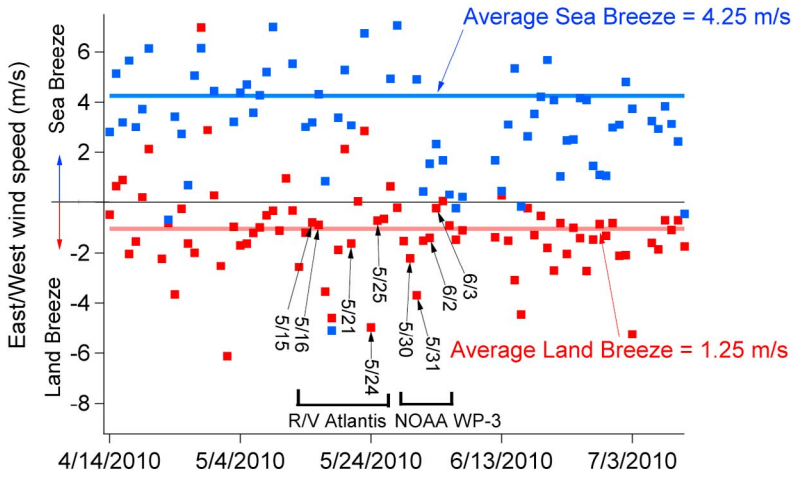

Figure 4. The consistency and strength of the sea breeze (blue) and the land breeze (red) is shown as the average east/west component of the wind velocity on each day. The averages are constructed from the LAX wind profiler data limited to the altitude range from 300 m to 600 m. The sea breeze is averaged between 5 P.M. and 8 P.M. and land breeze is averaged from 5 A.M. until 8 A.M. The arrows indicate nights during which the R/V Atlantis or the NOAA WP-3 was in Santa Monica Bay.

easterly component in the average, although an easterly flow was present on some individual nights.

[14] Above the surface, the sea breeze–land breeze circulation was a robust local weather pattern which occurs nearly every day. Figure 4 shows the average component of the wind velocity along an east-west direction. The averages were constructed using wind velocities between 300 m and 600 m measured by the wind profiler and averaging between 5 P.M. to 8 P.M. for the sea breeze (blue) and 5 A.M. to 8 A.M. for the land breeze (red). The average wind speeds of the land breeze and the sea breeze were 1.25 m/s and 4.25 m/s, respectively. Both the sea breeze and the land breeze are driven by the temperature difference between the sea and the land. The higher wind speeds in the sea breeze are consistent with larger temperature difference during the day than the night. The wind profiler reported data on 83 days of the 89-day averaging period. Out of those 83 days, the sea breeze (wind with a western component) was present 78 days (94%) and the land breeze (wind with an eastern component) was present on 69 nights (83%). Arrows in Figure 4 indicate the nights when either the R/V Atlantis or the NOAA WP-3 was sampling in Santa Monica Bay, and these nights were typical.

[15] The land breeze–sea breeze system over Santa Monica Bay is part of a larger circulation pattern common in the Los Angeles Bight. This is a counterclockwise circulation centered near Catalina Island. During episodes when this circulation is particularly strong it is called a Catalina Eddy [*Hu and Liu*, 2002; *Mass and Albright*, 1989; *Thompson et al.*, 1997; *Wakimoto*, 1987]. However, even when there is not a strong Catalina eddy, remnants of this circulation are evident especially at night when the sea breeze does not reduce the circulation. In addition to Santa Monica Bay, part of this circulation is observed in San Pedro Bay and along the coast of Orange County, where the nocturnal winds are typically parallel to the shore. These winds transport polluted urban air with recent emissions to Long Beach and the south side of the Palos Verdes peninsula. Aside from these regions of fresh urban outflow during the night (Santa Monica Bay and Orange County coast), the air in the Los Angeles Bight is characteristic of aged, dilute polluted air which has recirculated for a few days, especially when compared with cleaner air masses north of Point Conception.

4. Chemical Measurements and Analysis

[16] Primary and second pollutants, including $ClNO_2$ and its precursors were observed on four nights in Santa Monica Bay from the R/V Atlantis. (Although meteorological measurements were made on 15 May 2010, neither $ClNO_2$ nor N_2O_5 measurements were available for that night.) These four nights were used to construct diurnal averages of the chemical composition of the air masses in Santa Monica Bay, with a particular focus on compounds relevant to the nighttime chemistry occurring during the land breeze.

4.1. Nighttime Nitrogen Oxides and Halogens

[17] Figure 5 (top) shows the mixing ratios of O_3 (black) and NO_2 (green). The shaded areas show the 90th–10th percentiles of the data. When the land breeze developed around midnight, average NO_2 increased to 8 ppbv, while average O_3 decreased due to titration by recent NO emissions and by further reaction with NO_2 to produce NO_3 and N_2O_5. The average NO_2 mixing ratio began decreasing as the land breeze weakened and reversed around midday. In the afternoon during the sea breeze the average ozone mixing ratio increased to a maximum of 60 ppbv.

[18] Figure 5 (middle) shows the diurnally averaged $ClNO_2$ (blue) and N_2O_5 (red) mixing ratios. Both $ClNO_2$ and N_2O_5 were observed in the land breeze. After sunrise $ClNO_2$ concentrations decayed over four hours in the morning, consistent with its measured photolytic lifetime, which was ~7 h at 7 A.M., decreasing to 1 h at 10 A.M. Average N_2O_5 increased as the land breeze developed and peaked around 2 A.M. at

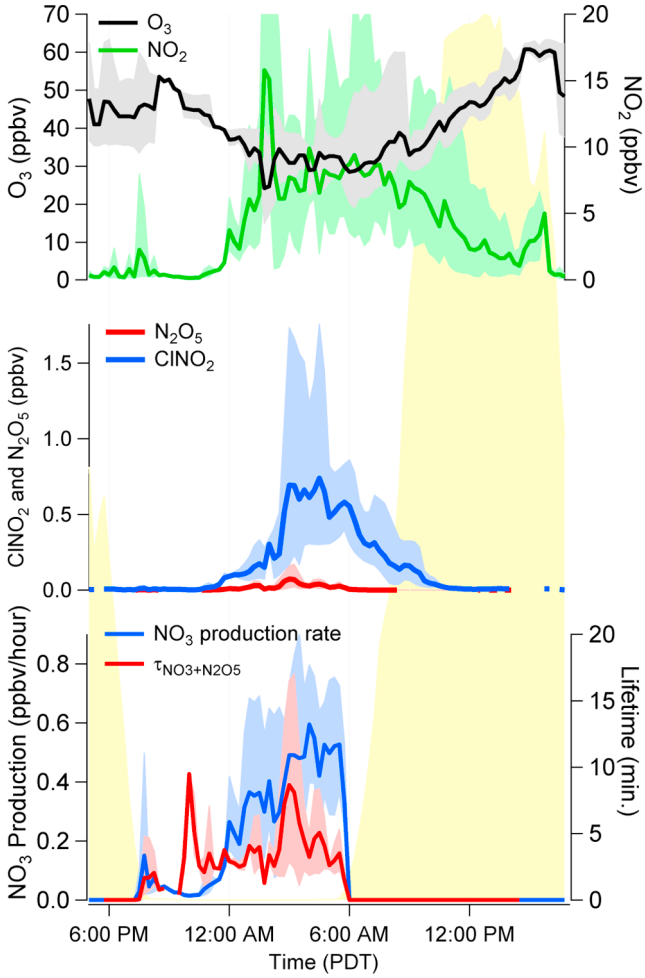

Figure 5. Diurnally averaged mixing ratios of $ClNO_2$ and its precursors. The averages are constructed from measurement made abroad the R/V Atlantis while it was in Santa Monica Bay. Shown is (top) the mixing ratios of O_3 (black) and NO_2 (green), (middle) $ClNO_2$ (blue) and N_2O_5 (red) mixing ratios, and (bottom) production rate of NO_3 (blue) and the summed lifetime (red) of NO_3 and N_2O_5. Shaded regions show the 10th–90th percentile of the measurements used in the average. The NO_2 photolysis rate (yellow) in the background indicates sunrise and sunset.

concentrations near 100 pptv. After sunrise the N_2O_5 concentration quickly decayed due to its short thermal lifetime (<10 s at 20°C) and rapid photolytic destruction of NO_3.

[19] Figure 5 (bottom) shows the NO_3 radical production rate (blue) and the lifetime (red) of the summed NO_3 and N_2O_5. Both the production rate and the lifetime are only calculated during the nighttime. The NO_3 radical production rate ($P(NO_3)$) in equation (1) is the product of the O_3 concentration, NO_2 concentration, and the rate constant for the reaction.

$$P(NO_3) = k_{O3+NO2}[O_3][NO_2] \quad (1)$$

[20] During the land breeze, the NO_3 production rate varied from 0.2 to 0.8 ppbv h^{-1}, a moderate to large value for urban air [*Aldener et al.*, 2006; *Geyer et al.*, 2001]. The average NO_3 and N_2O_5 mixing ratios, by contrast, were small, less than 5 pptv and 50 pptv, respectively. These observations imply rapid loss rates of either N_2O_5 or NO_3. This can be seen in the relatively short summed lifetime shown in Figure 5 (bottom) and defined in equation (2) as the sum of NO_3 and N_2O_5 concentration divided by the NO_3 production rate.

$$\tau_{NO3+N2O5} = \frac{[NO_3] + [N_2O_5]}{k_{O3+NO2}[O_3][NO_2]} \quad (2)$$

[21] During the land breeze, the average lifetime was never greater than 10 min. and was typically 5 min. Box model simulations of N_2O_5 (shown in Appendix A) show that N_2O_5 can rise to near steady state levels and in many cases achieve steady state during transport time from the coast to the R/V Atlantis alone.

[22] To fully characterize $ClNO_2$ production, three processes need to be quantified: the rate of NO_3 losses to reactions with VOCs, the N_2O_5 heterogeneous loss rate, and the yield of $ClNO_2$, which is the fraction of N_2O_5 heterogeneous loss that produces $ClNO_2$. The following two sections discuss the loss rates of NO_3 and N_2O_5, which are then integrated into a box model to constrain $ClNO_2$ production over water.

4.2. NO_3-VOC Reactions

[23] NO_3 is lost to reactions with biogenic volatile organic compounds (VOCs) and a few reactive anthropogenic VOCs. Mixing ratios of several VOCs were measured aboard the R/V Atlantis by proton transfer reaction time-of-flight mass spectrometry (PTR-ToF-MS) [*Jordan et al.*, 2009] and in situ gas chromatography instrument with flame-ionization detection (GC-FID) [*Kuster et al.*, 2004]. The measured VOCs included typical reaction partners for NO_3 such as isoprene, monoterpenes, dimethyl sulfide (DMS), and other common VOCs such as propane and propene. The pseudo first-order loss rate coefficient for the reaction of NO_3 with these VOCs was calculated using equation (3) for each species measured. Here, [VOC] is the measured concentrations of the VOC and $k_{VOC+NO3}$ is the rate constant for the reaction.

$$k_{NO3} = \sum k_{VOC+NO3}[VOC] \quad (3)$$

[24] In Figure 6 the average mixing ratio of dimethyl sulfide (DMS) is shown, which ranged from below the 18 pptv detection limit to 90 pptv in some instances (equivalent to NO_3 lifetimes of >37 min. to 4 min., respectively). Figure 6 (bottom) is a comparison of the loss rate coefficients due to reaction with DMS and the summed loss rate from all other measured VOCs. Over Santa Monica Bay the most important NO_3 loss was its reaction with DMS (orange). The summed loss rate coefficient from all other measured VOCs is shown in blue and is two to three orders of magnitude less than the loss rate coefficient from DMS. It is not expected that any unmeasured VOCs would compete with the DMS-NO_3 reaction in a marine environment. Prior analyses in other polluted marine environments have also shown that DMS is a dominant loss for NO_3 and that nighttime DMS oxidation by NO_3 is a dominant pathway for oxidation of marine sulfur [*Allan et al.*, 1999; *Osthoff et al.*, 2009; *Stark et al.*, 2007;

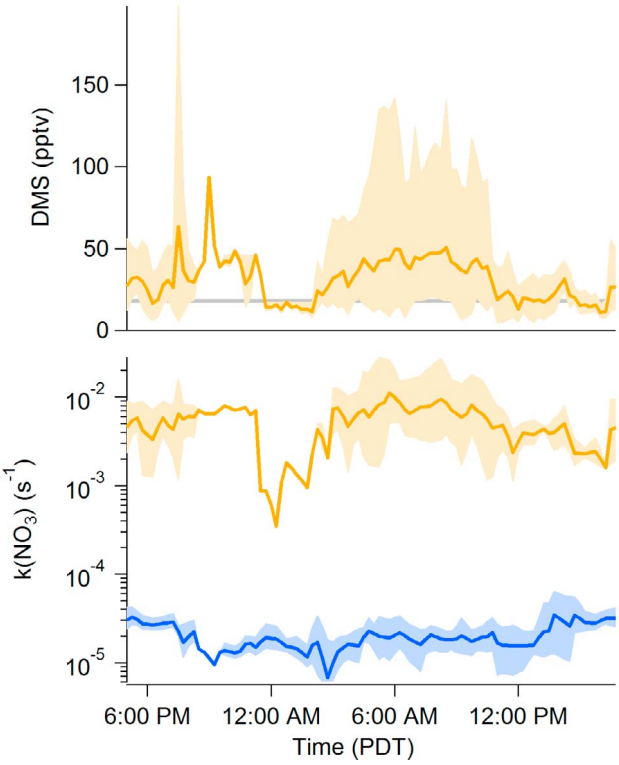

Figure 6. (top) The diurnally average mixing ratio of DMS (orange). The gray line at 18 pptv shows the detection limit of the instrument. The 90th through 10th percentile of the measurements used to construct the average are shown in the shaded region. (bottom) Also shown is the pseudo first-order loss rate coefficients for NO_3. The loss due to DMS is show in orange and the combined loss due to all other measured VOCs is shown in blue. The loss rate coefficients are calculated using VOC mixing ratios measured aboard the R/V Atlantis according to equation (3).

Vrekoussis et al., 2004; *Yvon et al.*, 1996]. Because there was only one VOC that dominated the NO_3 reactivity, this analysis will consider only NO_3 losses by reaction with DMS and neglect other VOCs.

4.3. N_2O_5 Heterogeneous Uptake

[25] The heterogeneous loss rate coefficient for N_2O_5 is determined by the aerosol surface area and the uptake coefficient as shown in equation (4), which has not been corrected for the effects of gas phase diffusion to the aerosol surfaces [*Fuchs and Stugnin*, 1970]; however, the gas phase diffusion correction is small (<10%) for particle distributions measured aboard the R/V Atlantis. Here k_{N2O5} is the pseudo first-order loss rate coefficient for N_2O_5, $\gamma(N_2O_5)$ is the uptake coefficient, $\bar{c}$ is the mean molecular speed of N_2O_5 (which varies weakly at ambient temperature), and A_s is the aerosol surface area density.

$$k_{N2O5} = \frac{\gamma(N_2O_5)\bar{c}A_S}{4} \quad (4)$$

[26] The N_2O_5 uptake coefficient is variable under ambient conditions depending aerosol composition and morphology [*Bertram et al.*, 2009; *Brown et al.*, 2006; *Chang et al.*, 2011]. In laboratory experiments, uptake of N_2O_5 is most efficient on pure water droplets and is reduced by the presence of nitrate and organics. The measurements of the uptake coefficient on water droplets ranges from 0.01 to 0.04 [*Bertram and Thornton*, 2009; *Hallquist et al.*, 2003; *Schutze and Herrmann*, 2002; *Schweitzer et al.*, 1998; *Van Doren et al.*, 1990]. Using the largest measured coefficient gives an upper limit to the amount of N_2O_5 taken up to the aerosol and subsequently an upper limit of the $ClNO_2$ production.

[27] An increase in aerosol number and mass was correlated with land breeze. The aerosol size distribution was measured and corrected using methods described by *Quinn et al.* [2002]. The particles were measured at 60% relative humidity (RH), and a growth factor based on the aerosol composition and the AeRho aerosol thermodynamic model [*Quinn and Coffman*, 1998] was used to correct the diameters to ambient RH. Typical growth factors (relative to 60% RH) ranged from 1 to 1.6 at 90% RH. The aerosol surface area density calculated from the corrected size distributions is shown as a diurnal average in Figure 7. The surface area density includes particles with aerodynamic diameters between 0.02 μm to 10 μm. Measured surface area density ranged from below 100 $\mu m^2/cm^3$ to greater than 400 $\mu m^2/cm^3$. Using the pure water N_2O_5 uptake coefficient (0.04) the surface can be converted into an upper-limit loss rate coefficient for N_2O_5 (equation (4)), shown on the left scale on Figure 7. In part because the heterogeneous N_2O_5 loss rate is relatively fast, the possible loss of N_2O_5 due to its homogeneous reaction with gas phase water has been omitted [*Wahner et al.*, 1998].

4.4. $ClNO_2$ Production Box Model

[28] Using the parameters determined in the preceding sections, a zero dimensional box model is used to calculate an upper limit to the amount of $ClNO_2$ produced during transport over water on the land breeze in Santa Monica Bay. To get the upper limit the $ClNO_2$ yield is taken to be 100% and the maximum N_2O_5 uptake coefficient 0.04 is used, rather than the Bertram and Thornton parameterization [*Bertram and Thornton*, 2009]. The maximum $ClNO_2$ production can then be compared to the observed $ClNO_2$ mixing ratios to determine the extent of possible $ClNO_2$ production over water. The box model includes six reactions (R3)–(R8). The combined rate of reactions (R7) and (R8) is determined by the N_2O_5 uptake coefficient, equation (4), and the rate of reaction (R8) is set to zero to give a $ClNO_2$ yield of 100%.

(R3) $$O_3 + NO_2 \rightarrow NO_3 + O_2$$

(R4) $$NO_3 + NO_2 \rightarrow N_2O_5$$

(R5) $$N_2O_5 \rightarrow NO_3 + NO_2$$

(R6) $$NO_3 + DMS \rightarrow HNO_3 + CH_3SCH_2$$

(R7) $$N_2O_5 + Cl^-(aq.) \rightarrow ClNO_2 + NO_3^-(aq.)$$

(R8) $$N_2O_5 + H_2O(aq.) \rightarrow 2HNO_3$$

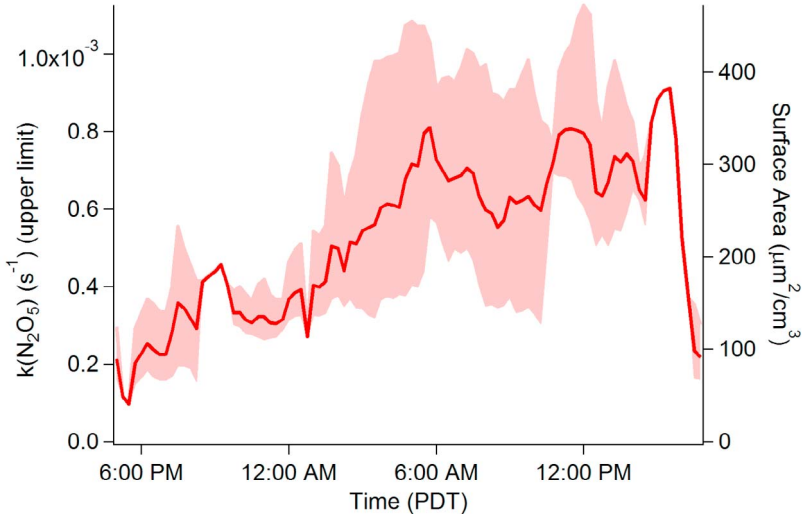

Figure 7. The diurnally averaged aerosol surface area density constructed from measured particle size distributions. The measured surface area includes particles ranging in diameter from 0.02 μm to 10 μm. The surface area density can be converted to upper limit for the N_2O_5 hydrolysis rate coefficient using equation (4) and an uptake coefficient of 0.04.

The same four nights used to construct the diurnal averages are chosen for box modeling. The wind speed and direction measured aboard the R/V Atlantis along with the distance from the coast are used to determine the transport time of air from the land to the ship. It is assumed that the air mass underwent only chemical transformation without dilution or mixing during this transport. During each night, time periods at the end of the night were selected. $ClNO_2$ concentrations for each night are shown in Appendix B. The box model was initialized to the average values of O_3, NO_2, and N_2O_5 during this time period. An example of the box model calculation is shown in Figure 8.

[29] The result of the box model for each of the four nights is shown in Figure 9. Details of each night modeled are in Table 2. On three of the four nights the upper limit of $ClNO_2$ production with a yield of 100% cannot account for the observed mixing ratio. These results indicate that a significant amount of $ClNO_2$ that had been formed within the terrestrial boundary layer over the Los Angeles Basin was transported over Santa Monica Bay in the land breeze. On 16 May, the only day the upper limit exceeds the observation, measurements of NO_z suggest that the actual yield was lower than 100% (see the next section). The source of chloride aerosol for the production of $ClNO_2$ over Los Angeles is likely the sea breeze which due to its higher wind speed is more efficient at transporting chloride aerosol inland than the weaker land breeze can transport urban NO_x offshore.

4.5. Estimating the $ClNO_2$ Yield

[30] When N_2O_5 is taken up on aerosol the yield of $ClNO_2$ depends on the competition between the reaction with chloride and the reaction with condensed water, and the yield can vary from 0% when no chloride is available to 100% when the chloride molarity is greater than 1 M. The yield has been parameterized in laboratory experiments as a function of nitrate, chloride, and water molarity [*Behnke et al.*, 1997; *Bertram and Thornton*, 2009; *Roberts et al.*, 2009]. In this analysis the yield is estimated using gas phase measurements of the products, $ClNO_2$ and a proxy for HNO_3. Although not done here, the yield could also be estimated using measurements of particulate chloride and the laboratory parameterizations. This method was not chosen because the measurements of chloride aboard R/V Atlantis did not include sea salt (nonrefractory chloride measured an aerosol mass spectrometer) or had poor time resolution (12 h filter-based measurement) which could not be well correlated to the land breeze.

[31] The $ClNO_2$ yield can be estimated by comparing the amount of nitric acid produced by nocturnal chemistry to the amount of $ClNO_2$ produced. The production of $ClNO_2$ begins with the production of the NO_3 by reaction (R1). Two branching points follow this source reaction. The first is the competition between loss of the NO_3 by reaction with VOCs or by conversion to N_2O_5 and its subsequent heterogeneous reactions. The second branching point is the competition between production of HNO_3 + $ClNO_2$ and 2 × HNO_3 from the reactive uptake of N_2O_5 (reactions (R7) and (R8)).

[32] The yield of the first branching point is the amount of N_2O_5 lost normalized by the total amount of both N_2O_5 and NO_3 lost. These amounts are expressed in terms of loss rate coefficients and concentrations in equation (5). This ratio can be simplified using equilibrium ratio of N_2O_5 to NO_3, given by $K_{eq}[NO_2]$ in equation (5) below. The yield as stated in equation (5) requires NO_3 and N_2O_5 to be in equilibrium with each other and in steady state with respect to production and loss of both NO_3 and N_2O_5, as shown in Appendix A.

$$\varepsilon = \frac{k_{N2O5}[N_2O_5]}{k_{NO3}[NO_3] + k_{N2O5}[N_2O_5]} = \frac{1}{1 + \frac{k_{NO3}}{k_{N2O5}} \frac{1}{K_{eq}[NO_2]}} \quad (5)$$

[33] Here ε is the fraction of NO_3 production that is lost through N_2O_5 compared to the total lost through both NO_3

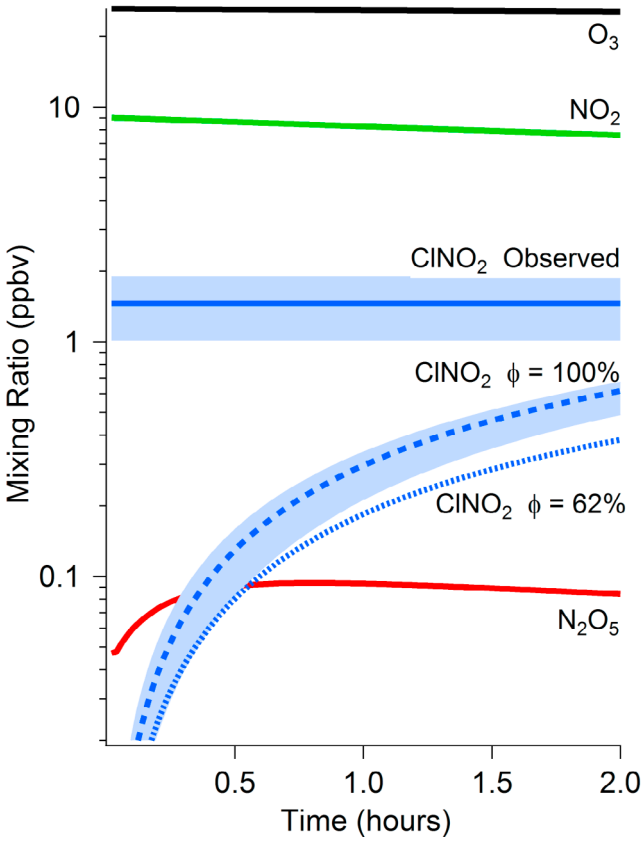

Figure 8. An example of the box model calculation of $ClNO_2$ production over water on the night of 21 May 2010. The time duration is the transport time from the coast to the R/V Atlantis. The solid blue line indicates the observed mixing ratio of $ClNO_2$ and the dashed line shows the upper limit of $ClNO_2$ production for yields of 100% and 62%. The light blue areas indicate the measurement uncertainty and the uncertainty in the calculated $ClNO_2$ mixing ratio.

and N_2O_5. Here k_{NO3} and k_{N2O5} are the loss rate coefficients for NO_3 and N_2O_5 discussed in the previous sections and K_{eq} is the equilibrium constant for the reaction of NO_3 and NO_2 to make N_2O_5. Because the loss rate coefficient for N_2O_5 calculated above is an upper limit, ε is also an upper limit. At the second branching point the $ClNO_2$ yield (Φ) depends on the composition and structure of aerosol.

[34] Other than $ClNO_2$ the main product of nocturnal nitrogen oxide chemistry is nitric acid (HNO_3). Since no measurements of HNO_3 were reported aboard the R/V Atlantis, $NO_z = NO_y - NO_x$ is the best available proxy for HNO_3. NO_z is mainly composed of HNO_3, $ClNO_2$, and HONO from nocturnal chemistry and HNO_3, peroxyacetyl nitrate, and organic nitrates produced by daytime photochemistry. For each night discussed below the O_3 was anticorrelated with NO_z (shown in Appendix C), suggesting that the NO_z is primarily nocturnal in origin. Nocturnal production of peroxyacetyl nitrate and organic nitrate is not expected in the marine environment because NO_3 reacts primarily with DMS, a reaction that converts the nitrogen into the form of HNO_3 [*Jensen et al.*, 1992]. The ratio of $ClNO_2$ to NO_z can be used to determine the yield of $ClNO_2$, when the loss of HNO_3 is slow such that HNO_3 is approximately conserved over the course of the night and any aerosol nitrate produced from hydrolysis of N_2O_5 is measured as NO_y whether it is in the aerosol or repartitioned into the gas phase as HNO_3. When these conditions are met, the slope (m) of the $ClNO_2$ versus NO_z correlation can be related to the yields from each branching point described above, equation (6).

$$
\begin{aligned}
m &= \frac{\Delta ClNO_2}{\Delta NO_z} \\
&= \frac{\Delta ClNO_2}{\Delta ClNO_2 + \Delta HNO_{3,R7} + \Delta HNO_{3,R8} + \Delta HNO_{3,R6}} \\
&= \frac{\varepsilon\Phi P_{NO3}}{\varepsilon\Phi P_{NO3} + \varepsilon\Phi P_{NO3} + 2\varepsilon(1-\Phi)P_{NO3} + (1-\varepsilon)P_{NO3}} \\
&= \frac{\varepsilon\Phi}{2\varepsilon\Phi + 2\varepsilon(1-\Phi) + (1-\varepsilon)} = \frac{\varepsilon\Phi}{1+\varepsilon}
\end{aligned}
\tag{6}
$$

[35] During nocturnal chemistry, changes in NO_z (ΔNO_z) have contributions from $ClNO_2$ and three sources of HNO_3. The heterogeneous reaction of N_2O_5 with chloride aerosol produces equimolar amounts of HNO_3 and $ClNO_2$ ($\Delta HNO_{3,R7}$). The heterogeneous reaction of N_2O_5 with aqueous water

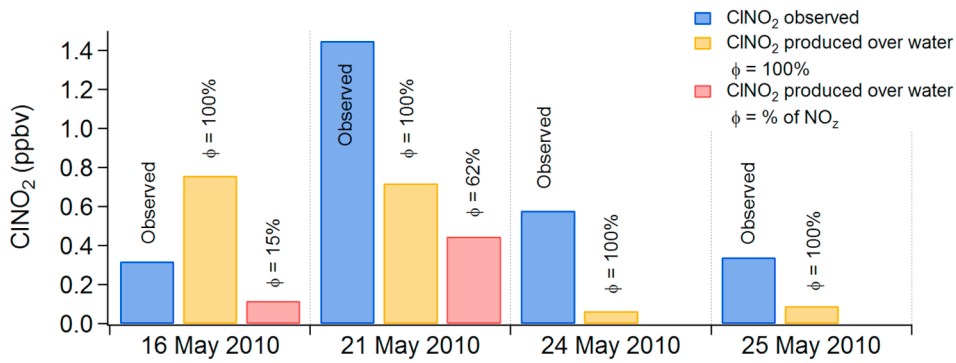

Figure 9. The results of a box model to calculate the upper limit of $ClNO_2$ production over water. Three of the four night the observation exceed the upper limit with a yield of 100% showing that a significant amounts of $ClNO_2$ are transported into Santa Monica Bay in the land breeze. For 16 and 21 May the red bar shows the amount of $ClNO_2$ produced using a smaller yield calculated from the slope of the $ClNO_2$ versus NO_z plot, equation (6).

Table 2. Parameters Used in the Box Model to Calculate an Upper Limit of $ClNO_2$ Production Over Water[a]

	16 May 2011	21 May 2011	24 May 2011	25 May 2011
Distance to the Coast	6.7 km	12.6 km	2.1 km	7.3 km
Transport time	1.8 h	2.0 h	0.18 h	1.1 h
N_2O_5	23 ± 6 pptv	49 ± 13 pptv	54 ± 19 pptv	8 ± 3 pptv
NO_2	9.4 ± 2.1 ppbv	9.0 ± 0.6 ppbv	14.3 ± 3.2 ppbv	3.2 ± 0.8 ppbv
O_3	35.5 ± 2.4 ppbv	26.4 ± 3.3 ppbv	21.5 ± 2.6 ppbv	34.8 ± 1.0 ppbv
DMS	35 ± 10 pptv	18 ± 11 pptv	21 ± 10 pptv	15 ± 9 ppbv
$k_{NO3+DMS}$	0.005 s^{-1}	0.0025 s^{-1}	0.0035 s^{-1}	0.0021 s^{-1}
Surface area ($\mu m^2/cm^3$)	421 ± 24	350 ± 35	240 ± 21	116 ± 10
k_{N2O5}	0.001 s^{-1}	0.0011 s^{-1}	0.0006 s^{-1}	0.0003 s^{-1}
$ClNO_2$ produced over water γ = 100%	650 pptv	545 pptv	49 pptv	39 pptv
ε	0.48	0.67		
Φ	15.4	62.0		
$ClNO_2$ produced over water γ = $ClNO_2$ versus NO_z	117 pptv	446 pptv		
$ClNO_2$ observed	320 pptv ± 45 pptv	1450 ± 250 pptv	580 ± 61 pptv	340 ± 41 pptv

[a]Observed $ClNO_2$ mixing ratios are also shown for comparison.

produces two HNO_3 molecules for each N_2O_5 molecule ($\Delta HNO_{3,R8}$), and the gas-phase reaction of NO_3 with DMS produces one HNO_3 ($\Delta HNO_{3,R6}$). When N_2O_5 and NO_3 are in steady state, each of these contributions can be quantified with the yields (ε and Φ) of the two branching points described above and is proportional to the total nitrate radical production (from $NO_2 + O_3$) integrated throughout the night (P_{NO3}). The $ClNO_2$ yield (Φ) can be determined using equation (6), the slope (m) from a plot of $ClNO_2$ versus NO_z, and branching between NO_3 and N_2O_5 (ε) from equation (5).

[36] For each night that was modeled, a plot of the $ClNO_2$ mixing ratios against NO_z mixing ratios (from 1:30 A.M. until 7 A.M.) is shown in Figure 10. On 16 May and 21 May, the mixing ratios of $ClNO_2$ and NO_z were well correlated; however, on 24 and 25 May there was no strong correlation. The lack of correlation on 24 and 25 May could be due to products of photochemistry making significant contributions to NO_z, or HNO_3 having a short and variable lifetime. Because of the strong correlation on 16 and 21 May, the slope was used to determine the $ClNO_2$ yield. On the 16 May,

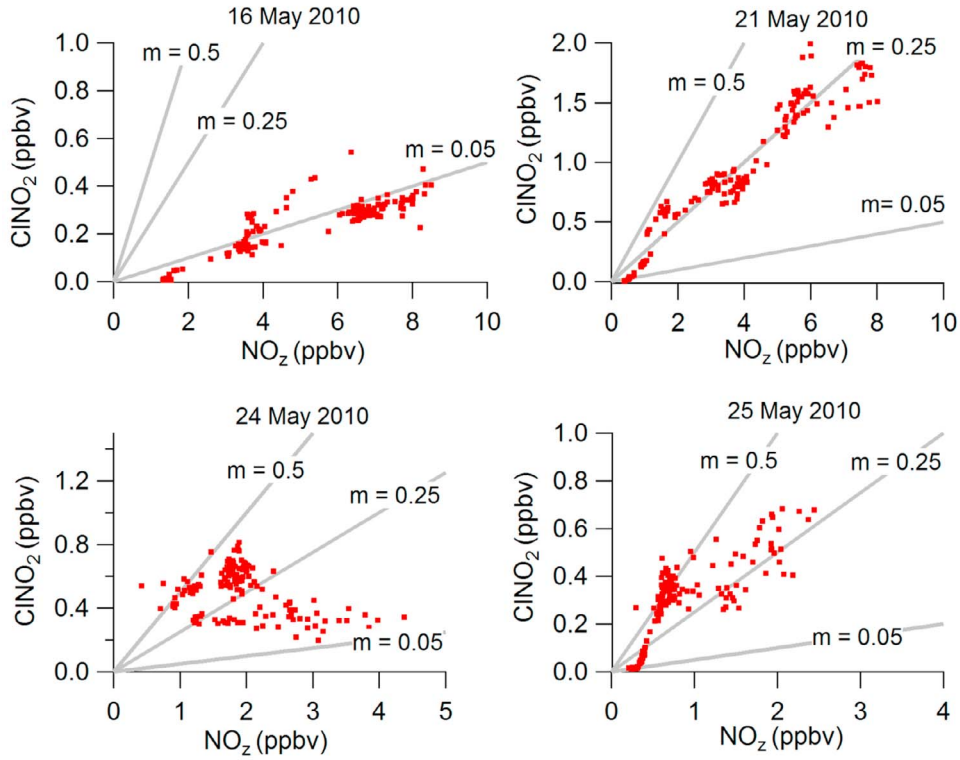

Figure 10. The ratio of $ClNO_2$ to NO_z gives an indication of the $ClNO_2$ yield from N_2O_5 hydrolysis. Plots of $ClNO_2$ against NO_z are shown for four nights during which the R/V Atlantis observed the land breeze in Santa Monica Bay. Gray lines show the slope which is used to determine the $ClNO_2$ yield in equation (6). For each night data collected between 1:30 A.M. and 7 A.M. is shown. Each data point represents the 1 min average mixing ratio.

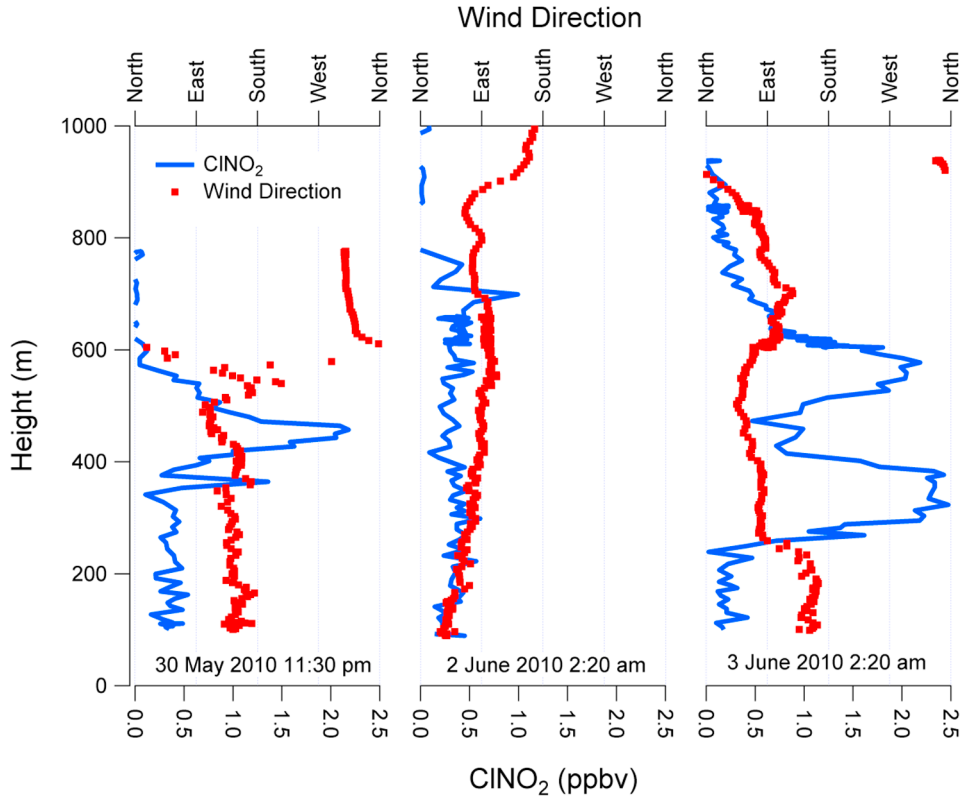

Figure 11. Vertical profiles of wind direction (red) and $ClNO_2$ (blue) mixing ratio measured over LAX aboard the NOAA WP-3 aircraft. All three profiles show the land breeze below 600 m where the wind direction has an easterly component. The profiles on 30 May and 3 June have layers where the $ClNO_2$ mixing ratio is greater than 2 ppbv. Additionally below these layers and in the 2 June profile, the $ClNO_2$ mixing ratio is between 0.1 and 0.5 ppbv. Above the land breeze, greater than 800 m, the $ClNO_2$ mixing ratio drops below the instrument detection limit.

the slope was $m = 0.05$ and the branching between NO_3 and N_2O_5 was $\varepsilon = 0.48$ giving a $ClNO_2$ yield of 15.4%. On 21 May, the $ClNO_2$ yield was 62% from a slope of $m = 0.25$ and the branching of $\varepsilon = 0.67$.

[37] There are several difficulties and unknowns when determining the $ClNO_2$ yield using the method described above. First, this method assumes the all air masses sampled begin the night with the same amount of NO_y before nocturnal chemistry makes any contribution. Second, HNO_3 may not be conserved. The HNO_3 lifetime is estimated based on the marine boundary layer depth (500–700 m) and a typical marine deposition velocity (1.2 cm/s) to be 11–16 h. If an air mass were over water the entire night (~10 h) this would lead to a 50% to 60% loss of HNO_3. However, if the air masses are transported to R/V Atlantis above the surface and mixed down to the surface after crossing the coast, as described by *Shair et al.* [1982], then HNO_3 loss to the surface by deposition could be smaller. Third, the air masses transported to the R/V Atlantis may have different partitioning between the HNO_3 and particulate nitrate. If the NO_y measurement does not sample HNO_3 and particulate NO_3^- with the same efficiency, a change in this partitioning leads to gain or loss of NO_z not associated with N_2O_5 uptake. Measurements of particulate NO_3^- concentration during the land breeze were less than 20% of NO_z concentration and would reduce the estimated yield. Fourth, HONO was not measured aboard the R/V Atlantis. If its concentration were proportional to NO_z it would lead to an under estimation of $ClNO_2$ yield. In spite of these difficulties in determining the yield, on 16 March the slope of the $ClNO_2$ against NO_z suggests the $ClNO_2$ yield is significantly lower than 100% and that on all four nights analyzed here $ClNO_2$ is produced over land and transported to Santa Monica Bay.

5. Aircraft Vertical Profiles at LAX

[38] The transport of $ClNO_2$ in the land breeze is further confirmed by vertical profiles of $ClNO_2$ mixing ratio and wind direction over LAX measured aboard the NOAA WP-3 aircraft. The NOAA WP-3 flight track includes several missed approaches at airports around the Los Angeles Basin. The missed approaches are used to study the vertical variation of atmospheric composition and meteorology. There were missed approaches at LAX along the coast of Santa Monica Bay on three nights: 30 May, 2 June, and 3 June. Unfortunately, these nights do not overlap with nights the R/V Atlantis was also there, so a direct comparison is not possible. However, the strength of the land breeze was similar on the nights that the R/V Atlantis and the NOAA P-3 observed it, as shown in Figure 4.

[39] Figure 11 shows the vertical profiles of wind direction and $ClNO_2$ mixing ratio over LAX for each of the three flights.

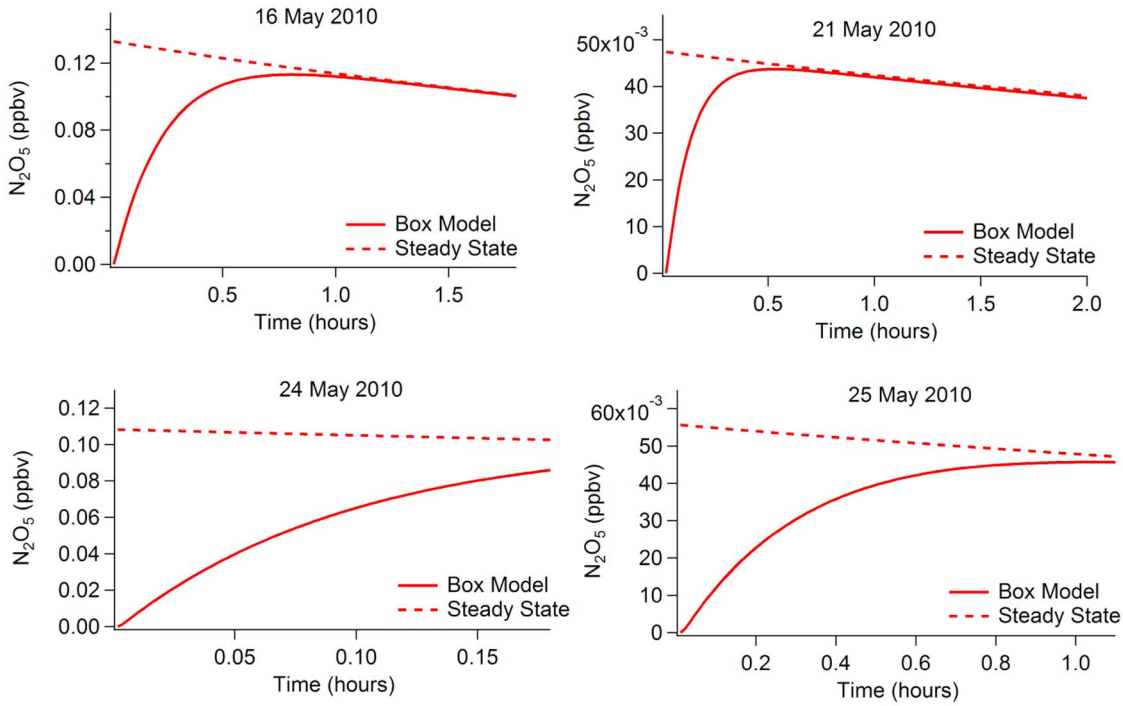

Figure A1. Box model results showing the N_2O_5 concentration approaching to steady state during each of the four nights analyzed.

In all three profiles there was an easterly component of the wind direction in the residual boundary layer. For each profile in residual boundary layer the wind speed (not shown) was between 2 m/s and 5 m/s. On 30 May, the residual boundary layer extended up to 600 m, and on 2 June the residual boundary layer depth was 800 m. The boundary layer was more complicated on 3 June. The wind was out of the east-northeast in a layer between 300 and 700 m, and below 300 m the wind was out of the southeast. The residual boundary layer in each profile is associated with an enhancement of the carbon monoxide, a typical tracer of urban air masses. Each of these profiles also shows $ClNO_2$ in the residual boundary layer being transported from the city to Santa Monica Bay in the land breeze. The profiles on 30 May and 3 June exhibit layers in which the mixing ratio of $ClNO_2$ exceeded 2 ppbv, and below these layers the $ClNO_2$ mixing ratio was 350 pptv on the 30 May and 200 pptv on 3 June. On 2 June, the nighttime boundary layer was well mixed, and the resulting potential temperature structure (not shown) indicated no inversions below 800 m. On this night, the $ClNO_2$ mixing ratio was between 100 and 500 pptv throughout this nocturnal/marine boundary layer below 800 m. These vertical profiles directly show the transport of $ClNO_2$ over Santa Monica Bay. The transport of urban air pollution and $ClNO_2$ was strongest in layers above the surface, consistent with the land breeze analysis from the wind profiler described in section 3.

6. Conclusions

[40] During nighttime when the R/V Atlantis and NOAA WP-3 were in Santa Monica Bay, the land breeze was responsible for transporting polluted urban air from the Los Angeles Basin out over Santa Monica Bay. The transport was most active in a layer 300 to 700 m above the surface. High concentrations of $ClNO_2$ were observed in this urban outflow. Although the marine environment represents an abundant source of chloride in the form of sea salt, most of the production of $ClNO_2$ took place over land, and a portion was transported to Santa Monica Bay in the land breeze. The ocean is likely the ultimate source of chloride for a large portion of the $ClNO_2$ production. The aerosol chloride is transported inland on the sea breeze, $ClNO_2$ is produced over the city, and a portion of that chloride returns in the early morning during the land breeze. Further study is needed to determine the frequency, seasonality, and intensity of this transport and the $ClNO_2$ formation. Similar transport and $ClNO_2$ production mechanisms are likely in other cities along the west coast of United States. However, on the east coast and gulf coast prevailing westerlies would transport NO_x over water more efficiently than the land breeze in Santa Monica, and more significant $ClNO_2$ production would then be expected over water.

Appendix A

[41] For the nights described in this work, the lifetime of N_2O_5 and NO_3 is short, never greater than 20 min and typically less than 10 min. It is unlikely NO or NO_2 are emitted into the observed air masses during transport over water. A box model is used to determine if enough time has elapsed during this unperturbed transport from the coast for N_2O_5 to come to steady state. The box model is the same as the model describe in the main text except that the N_2O_5 initial concentration (the concentration at the coast) was set to zero, instead of the value observed aboard the R/V Atlantis (which is used to determine the upper limit of $ClNO_2$ production). The N_2O_5

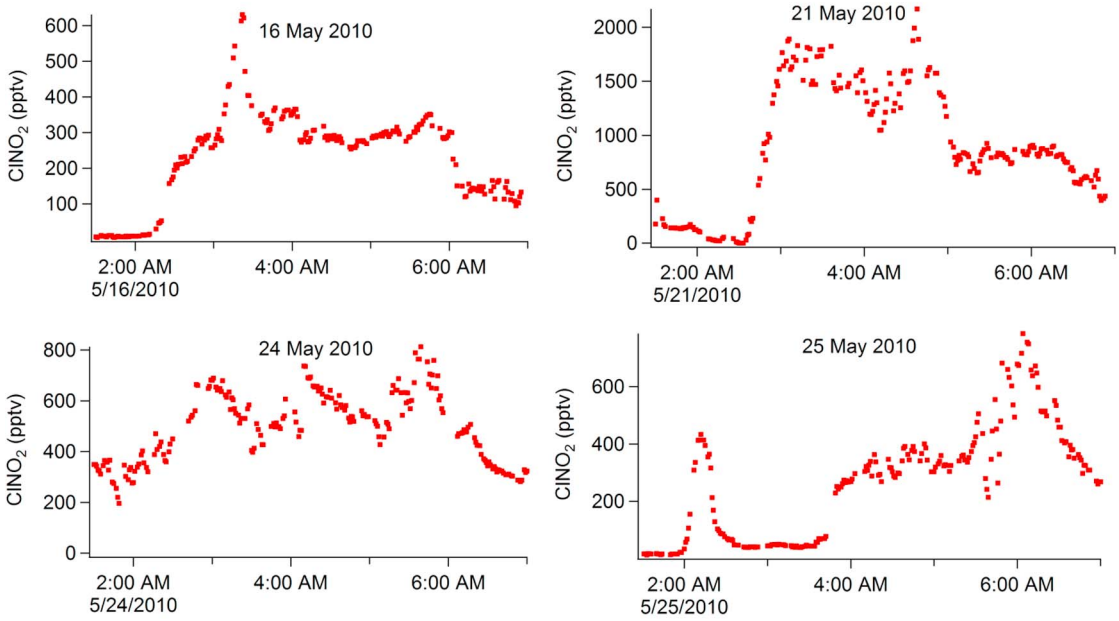

Figure B1. Four nights of $ClNO_2$ mixing ratios measured from the R/V Atlantis during the land breeze in Santa Monica Bay.

concentrations from this model are shown in Figure A1 along with a steady state concentration calculated with equation (A1), plotted against transport time from the coast.

$$[N_2O_5]_{SS} = \frac{k_{O3+NO2}[NO_2][O_3]}{\left(\frac{k_{NO3}}{K_{eq}[NO_2]} + k_{N2O5}\right)} \quad \text{(A1)}$$

[42] The loss rate coefficients used for k_{NO3} and k_{N2O5} are those estimated in the main text. On the nights of 16 and 21 May, the box model concentration rose to the steady state value well before the air mass was observed aboard the R/V Atlantis. On the nights of 24 and 25 May, the N_2O_5 concentration had not achieved steady state but was within 15% and 4% of the steady state values, respectively. The large concentration of $ClNO_2$ observed suggests the N_2O_5

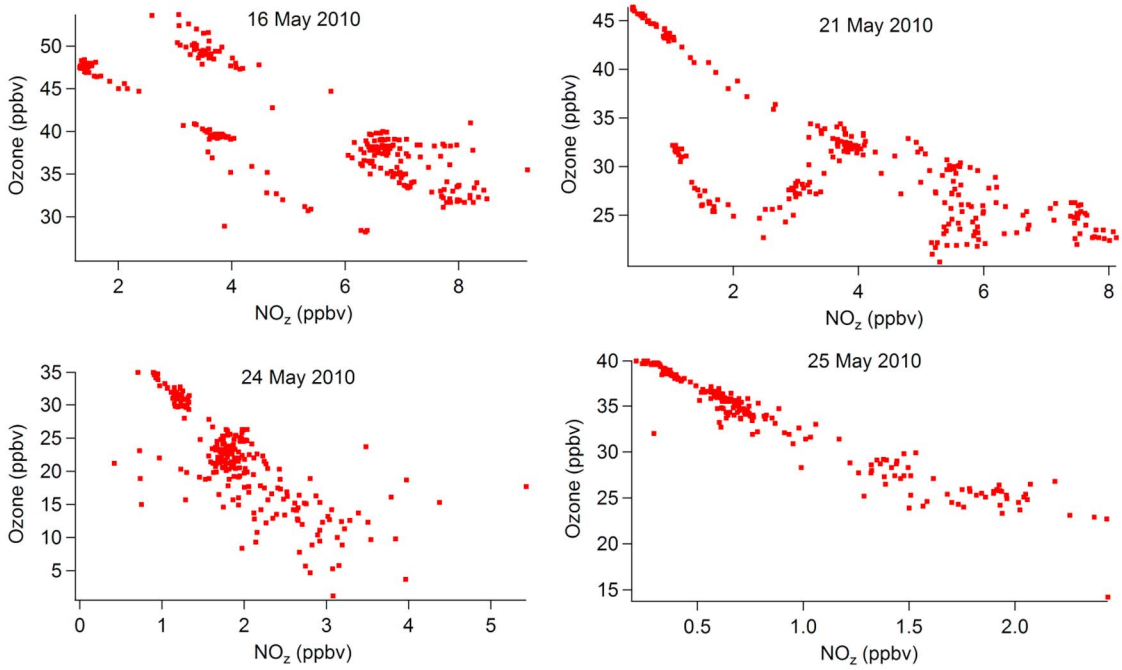

Figure C1. Ozone plotted against NO_z for each night used in the analysis. On each night, ozone is anticorrelated with NO_z.

concentrations were greater than zero at the coast, and if this was the case, it would take less time to achieve steady state.

Appendix B

[43] Time series of $ClNO_2$ for each night analyzed are shown in Figure B1. The time period plotted is 1:00 A.M. through 07:00 A.M., which is the time during which the land breeze was observed in Santa Monica Bay. The time periods which were used in the model are 3:30–5:00 A.M. on 16 May, 4:00–5:00 A.M. on 21 May, and 4:00–5:30 A.M. on 24 and 25 May.

Appendix C

[44] For each of the four analyzed nights, ozone is plotted as a function of NO_z in Figure C1. On each of these nights the ozone mixing ratio is anticorrelated with NO_z. Components of NO_z produced through photochemistry are expected to be correlated with higher ozone concentrations. Nocturnal components of NO_z produced by reactions with NO_3 and N_2O_5 are expected to be anticorrelated with NO_z because the production of NO_3 and N_2O_5 during the night consumes ozone. Additionally, direct emissions of NO_x are usually in the form of NO and consume ozone when converted to NO_2. Figure S2 shows that during the land breeze in Santa Monica Bay, ozone is consistently anticorrelated with NO_z indicating the NO_z originates from nocturnal NO_3 and N_2O_5 chemistry.

[45] **Acknowledgments.** We thank Kevin Durkee and the South Coast Air Quality Management district for providing data from the LAX wind profiler.

References

Aldener, M., et al. (2006), Reactivity and loss mechanisms of NO_3 and N_2O_5 in a polluted marine environment: Results from in situ measurements during New England Air Quality Study 2002, *J. Geophys. Res.*, *111*, D23S73, doi:10.1029/2006JD007252.

Allan, B. J., N. Carslaw, H. Coe, R. A. Burgess, and J. M. C. Plane (1999), Observations of the nitrate radical in the marine boundary layer, *J. Atmos. Chem.*, *33*(2), 129–154, doi:10.1023/A:1005917203307.

Behnke, W., C. George, V. Scheer, and C. Zetzsch (1997), Production and decay of $ClNO_2$, from the reaction of gaseous N_2O_5 with NaCl solution: Bulk and aerosol experiments, *J. Geophys. Res.*, *102*(D3), 3795–3804, doi:10.1029/96JD03057.

Bertram, T. H., and J. A. Thornton (2009), Toward a general parameterization of N_2O_5 reactivity on aqueous particles: The competing effects of particle liquid water, nitrate, and chloride, *Atmos. Chem. Phys.*, *9*(21), 8351–8363, doi:10.5194/acp-9-8351-2009.

Bertram, T. H., J. A. Thornton, T. P. Riedel, A. M. Middlebrook, R. Bahreini, T. S. Bates, P. K. Quinn, and D. J. Coffman (2009), Direct observations of N_2O_5 reactivity on ambient aerosol particles, *Geophys. Res. Lett.*, *36*, L19803, doi:10.1029/2009GL040248.

Boucouvala, D., R. Bornstein, J. Wilkinson, and D. Miller (2003), MM5 simulations of a SCOS97-NARSTO episode, *Atmos. Environ.*, *37*, 95–117, doi:10.1016/S1352-2310(03)00384-4.

Brown, S. S., et al. (2006), Variability in nocturnal nitrogen oxide processing and its role in regional air quality, *Science*, *311*(5757), 67–70, doi:10.1126/science.1120120.

Cass, G. R., and F. H. Shair (1984), Sulfate accumulation in a sea breeze land breeze circulation system, *J. Geophys. Res.*, *89*(D1), 1429–1438, doi:10.1029/JD089iD01p01429.

Chameides, W. L. (1978), Photo-chemical role of tropospheric nitrogen-oxides, *Geophys. Res. Lett.*, *5*(1), 17–20, doi:10.1029/GL005i001p00017.

Chang, W. L., P. V. Bhave, S. S. Brown, N. Riemer, J. Stutz, and D. Dabdub (2011), Heterogeneous atmospheric chemistry, ambient measurements, and model calculations of N_2O_5: A review, *Aerosol Sci. Technol.*, *45*(6), 665–695, doi:10.1080/02786826.2010.551672.

Finlayson Pitts, B. J., M. J. Ezell, and J. N. Pitts (1989), Formation of chemically active chlorine compounds by reactions of atmospheric NaCl particles with gasous N_2O_5 and $ClONO_2$, *Nature*, *337*(6204), 241–244, doi:10.1038/337241a0.

Fuchs, N. A., and A. G. Stugnin (1970), *Highly Dispersed Aerosol*, Ann Arbor Sci., Ann Arbor, Mich.

Gentner, D. R., R. A. Harley, A. M. Miller, and A. H. Goldstein (2009), Diurnal and seasonal variability of gasoline-related volatile organic compound emissions in Riverside, California, *Environ. Sci. Technol.*, *43*(12), 4247–4252, doi:10.1021/es9006228.

Geyer, A., B. Alicke, S. Konrad, T. Schmitz, J. Stutz, and U. Platt (2001), Chemistry and oxidation capacity of the nitrate radical in the continental boundary layer near Berlin, *J. Geophys. Res.*, *106*(D8), 8013–8025, doi:10.1029/2000JD900681.

Hallquist, M., D. J. Stewart, S. K. Stephenson, and R. A. Cox (2003), Hydrolysis of N_2O_5 on sub-micron sulfate aerosols, *Phys. Chem. Chem. Phys.*, *5*(16), 3453–3463, doi:10.1039/b301827j.

Hu, H., and W. T. Liu (2002), QuikSCAT reveals the surface circulation of the Catalina Eddy, *Geophys. Res. Lett.*, *29*(17), 1821, doi:10.1029/2001GL014203.

Jensen, N. R., J. Hjorth, C. Lohse, H. Skov, and G. Restelli (1992), Products and mechanisms of the gas-phase reactions of NO_3 with CH_3SCH_3, CD_3SCD_3, CH_3SH and CH_3SSCH_3, *J. Atmos. Chem.*, *14*(1–4), 95–108, doi:10.1007/BF00115226.

Jordan, A., S. Haidacher, G. Hanel, E. Hartungen, L. Mark, H. Seehauser, R. Schottkowsky, P. Sulzer, and T. D. Mark (2009), A high resolution and high sensitivity proton-transfer-reaction time-of-flight mass spectrometer (PTR-TOF-MS), *Int. J. Mass Spectrom.*, *286*(2–3), 122–128, doi:10.1016/j.ijms.2009.07.005.

Kercher, J. P., T. P. Riedel, and J. A. Thornton (2009), Chlorine activation by N_2O_5: Simultaneous, in situ detection of $ClNO_2$ and N_2O_5 by chemical ionization mass spectrometry, *Atmos. Meas. Tech.*, *2*(1), 193–204, doi:10.5194/amt-2-193-2009.

Kuster, W. C., B. T. Jobson, T. Karl, D. Riemer, E. Apel, P. D. Goldan, and F. C. Fehsenfeld (2004), Intercomparison of volatile organic carbon measurement techniques and data at la porte during the TexAQS2000 Air Quality Study, *Environ. Sci. Technol.*, *38*(1), 221–228, doi:10.1021/es034710r.

Mass, C. F., and M. D. Albright (1989), Origin of the Catalina eddy, *Mon. Weather Rev.*, *117*(11), 2406–2436, doi:10.1175/1520-0493(1989)117<2406:OOTCE>2.0.CO;2.

McLaren, R., P. Wojtal, D. Majonis, J. McCourt, J. D. Halla, and J. Brook (2010), NO_3 radical measurements in a polluted marine environment: Links to ozone formation, *Atmos. Chem. Phys.*, *10*(9), 4187–4206, doi:10.5194/acp-10-4187-2010.

Mielke, L. H., A. Furgeson, and H. D. Osthoff (2011), Observation of ClNO2 in a Mid-Continental Urban Environment, *Environ. Sci. Technol.*, *45*(20), 8889–8896, doi:10.1021/es201955u.

Osthoff, H. D., et al. (2008), High levels of nitryl chloride in the polluted subtropical marine boundary layer, *Nat. Geosci.*, *1*(5), 324–328, doi:10.1038/ngeo177.

Osthoff, H. D., et al. (2009), Regional variation of the dimethyl sulfide oxidation mechanism in the summertime marine boundary layer in the Gulf of Maine, *J. Geophys. Res.*, *114*, D07301, doi:10.1029/2008JD010990.

Pollack, I. B., B. M. Lerner, and T. B. Ryerson (2010), Evaluation of ultraviolet light-emitting diodes for detection of atmospheric NO_2 by photolysis-chemiluminescence, *J. Atmos. Chem.*, *65*(2–3), 111–125, doi:10.1007/s10874-011-9184-3.

Quinn, P. K., and D. J. Coffman (1998), Local closure during the First Aerosol Characterization Experiment (ACE 1), Aerosol mass concentration and scattering and backscattering coefficients, *J. Geophys. Res.*, *103*(D13), 16,575–16,596, doi:10.1029/97JD03757.

Quinn, P. K., D. J. Coffman, T. S. Bates, T. L. Miller, J. E. Johnson, E. J. Welton, C. Neususs, M. Miller, and P. J. Sheridan (2002), Aerosol optical properties during INDOEX 1999: Means, variability, and controlling factors, *J. Geophys. Res.*, *107*(D19), 8020, doi:10.1029/2000JD000037.

Riedel, T. P., et al. (2012), Nitryl chloride and molecular chlorine in the coastal marine boundary layer, *Environ. Sci. Technol.*, *46*, 10,463–10,470, doi:10.1021/es204632r.

Roberts, J. M., H. D. Osthoff, S. S. Brown, A. R. Ravishankara, D. Coffman, P. Quinn, and T. Bates (2009), Laboratory studies of products of N_2O_5 uptake on Cl^- containing substrates, *Geophys. Res. Lett.*, *36*, L20808, doi:10.1029/2009GL040448.

Schutze, M., and H. Herrmann (2002), Determination of phase transfer parameters for the uptake of HNO_3, N_2O_5, and O_3 on single aqueous drops, *Phys. Chem. Chem. Phys.*, *4*(1), 60–67, doi:10.1039/b106078n.

Schweitzer, F., P. Mirabel, and C. George (1998), Multiphase chemistry of N_2O_5, $ClNO_2$, and $BrNO_2$, *J. Phys. Chem. A*, *102*(22), 3942–3952, doi:10.1021/jp980748s.

Shair, F. H., E. J. Sasaki, D. E. Carlan, G. R. Cass, W. R. Goodin, J. G. Edinger, and G. E. Schacher (1982), Transport and dispersion of airborne

pollutants associated with the land breeze sea breeze system, *Atmos. Environ.*, *16*(9), 2043–2053, doi:10.1016/0004-6981(82)90275-X.

Stark, H., S. S. Brown, P. D. Goldan, M. Aldener, W. C. Kuster, R. Jakoubek, F. C. Fehsenfeld, J. Meagher, T. S. Bates, and A. R. Ravishankara (2007), Influence of nitrate radical on the oxidation of dimethyl sulfide in a polluted marine environment, *J. Geophys. Res.*, *112*, D10S10, doi:10.1029/2006JD007669.

Thompson, W. T., S. D. Burk, and J. Rosenthal (1997), An investigation of the Catalina eddy, *Mon. Weather Rev.*, *125*(6), 1135–1146, doi:10.1175/1520-0493(1997)125<1135:AIOTCE>2.0.CO;2.

Thornton, J. A., et al. (2010), A large atomic chlorine source inferred from mid-continental reactive nitrogen chemistry, *Nature*, *464*(7286), 271–274, doi:10.1038/nature08905.

Van Doren, J. M., L. R. Watson, P. Davidovits, D. R. Worsnop, M. S. Zahniser, and C. E. Kolb (1990), Temperature-dependence of the uptake coefficients of HNO_3, HCl, and N_2O_5 by water droplets, *J. Phys. Chem.*, *94*(8), 3265–3269, doi:10.1021/j100371a009.

Vrekoussis, M., M. Kanakidou, N. Mihalopoulos, P. J. Crutzen, J. Lelieveld, D. Perner, H. Berresheim, and E. Baboukas (2004), Role of the NO_3 radicals in oxidation processes in the eastern Mediterranean troposphere during the MINOS campaign, *Atmos. Chem. Phys.*, *4*, 169–182, doi:10.5194/acp-4-169-2004.

Wagner, N. L., W. P. Dube, R. A. Washenfelder, C. J. Young, I. B. Pollack, T. B. Ryerson, and S. S. Brown (2011), Diode laser-based cavity ring-down instrument for NO_3, N_2O_5, NO, NO_2 and O_3 from aircraft, *Atmos. Meas. Tech.*, *4*, 1227–1240, doi:10.5194/amt-4-1227-2011.

Wahner, A., T. F. Mentel, and M. Sohn (1998), Gas-phase reaction of N_2O_5 with water vapor: Importance of heterogeneous hydrolysis of N_2O_5 and surface desorption of HNO_3 in a large Teflon chamber, *Geophys. Res. Lett.*, *25*(12), 2169–2172, doi:10.1029/98GL51596.

Wakimoto, R. M. (1987), The Catalina eddy and its effect on pollution over southern California, *Mon. Weather Rev.*, *115*(4), 837–855, doi:10.1175/1520-0493(1987)115<0837:TCEAIE>2.0.CO;2.

Washenfelder, R. A., et al. (2011), The glyoxal budget and its contribution to organic aerosol for Los Angeles, California during CalNex 2010, *J. Geophys. Res.*, *116*, D00V02, doi:10.1029/2011JD016314.

Williams, E. J., F. C. Fehsenfeld, B. T. Jobson, W. C. Kuster, P. D. Goldan, J. Stutz, and W. A. McCleanny (2006), Comparison of ultraviolet absorbance, chemiluminescence, and DOAS instruments for ambient ozone monitoring, *Environ. Sci. Technol.*, *40*(18), 5755–5762, doi:10.1021/es0523542.

Williams, E. J., B. M. Lerner, P. C. Murphy, S. C. Herndon, and M. S. Zahniser (2009), Emissions of NO_x, SO_2, CO, and HCHO from commercial marine shipping during Texas Air Quality Study (TexAQS) 2006, *J. Geophys. Res.*, *114*, D21306, doi:10.1029/2009JD012094.

Yvon, S. A., J. M. C. Plane, C. F. Nien, D. J. Cooper, and E. S. Saltzman (1996), Interaction between nitrogen and sulfur cycles in the polluted marine boundary layer, *J. Geophys. Res.*, *101*(D1), 1379–1386, doi:10.1029/95JD02905.